Anal. Bioanal. Electrochem., Vol. 14, No. 12, 2022, 1114-1125

Analytical &
Bioanalytical
Electrochemistry

2022 by CEE
www.abechem.com

Full Paper

Electroanalytical Detection of Uric Acid on Blue HEGN Modified Glassy Carbon Electrode by Voltammetry

S. D. Sukanya,[1] B. E. Kumara Swamy,[2,*] and J. K. Shashikumara[2]

[1]*Department of P. G. Studies and Research in Analytical Chemistry, Alva's College, Moodubidire, Dakshina Kannada, Karnataka, 574227, India*
[2]*Department of P. G. Studies and Research in Industrial Chemistry, Kuvempu University, JnanaShyadri, Shankaraghatta, Shivmoga, Karnataka, 577451, India*

*Corresponding Author, Tel.: +91-8282-256225
E-Mail: kumaraswamy21@yahoo.com

Received: 31 October 2022 / Received in revised form: 22 December 2022 /
Accepted: 22 December 2022 / Published online: 31 December 2022

Abstract- An electroanalytical technique was advanced for the detection of uric acid (URI) relying on its oxidation behaviour. Using cyclic voltammetry (CV) techniques, the electrochemical performance and detection of URI were easily accomplished on poly (Blue HEGN) modified glassy carbon electrode (Po-BHEGN/GCE). The role of pH on anodic peak current and potential was examined. Phosphate buffer of 7.4 pH was opted for subsequent data analysis. Sweep rate studies were carried out and showed that electrode reaction was a diffusion-controlled process. A linear calibration curve was established in the URI concentration levels from 10-70 µM. The LOD and LOQ were estimated to be 0.94 and 2.91 µM, respectively. A simultaneous study of URI and dopamine (DA) revealed that well-separated peak at Po-BHEGN/GCE compare to GCE. To sum up, a straightforward and inexpensive sensor Po-BHEGN/GCE is built for the sensitive and focused detection of URI in samples.

Keywords- Uric acid; Blue HEGN; Glassy carbon electrode; Electroplolymerization; Cyclic Voltammetry

1. INTRODUCTION

Electroanalytical approaches, which rely on the interplay of electrical energy and matter and have lately emerged as a notable analytical technique for detecting constituents contained in a sample. Various voltammetric methods with their simplicity and high sensitivity can easily predict the electro-active compounds. All voltammetric methods prioritize the selection of the best operating electrode material [1,2]. The GCE is a valuable conductive material with a specific surface configuration, a broad operational window, selectivity and sensitivity in the findings, strong mechanical properties, and is easy to modify [3–6]. In the existence of interferences, the untreated GCE does not demonstrate the considerable and selective differentiation of electroactive [7–10]. Electrochemical researchers, on the other hand, have revealed that surface modification of an electrode is significant for boosting selectivity in detecting electrochemically active molecules. There are various publications in the literature on the electropolymerization of GCE, which led to the invention of electrodes such as poly(o-aminophenol) [11], poly (neutral red) [12], poly (allura red) [13], poly (glutamic acid) [14], poly (PEDOT) [15] and poly (AHNSA) [16].

URI is a waste product produced by the digestion of purine–containing foodstuff. URI is a significant by-product of purine metabolism. Typically, it stays within a stable range in healthy people [17–19]. The Kidneys dispose of around 70% of daily URI as a by-product of urine, while the balance is recirculated back into the bloodstream [20]. The typical blood URI content in healthy people is 3-7 mg/dL, while the amount discharged in the urine is approximately 16-100mg/dL every 24 hours [21–23]. An excessive purine intake from food causes the body to release an excessive amount of URI. Excess URI concentrates and crystallizes, leading to various disorders. The deposition of URI crystallizes in human joints causing gout. Furthermore, chronic renal, and cardiovascular diseases, Lesch-Nyan syndrome, and hepatitis are all linked to high URI levels [24–26]. An incredibly low URI level also can lead to other disorders including Sclerosis [27].

In other words, Changes in URI level might cause physiological ailments. The quantitative amount of URI is critical for therapeutic purposes such as diagnosis and medication management. URI generally co-exists with DA in blood and urine [28,29]. This behaviour poses a unique challenge in distinguishing URI from DA. As a result, the design of a sensor with excellent sensitivity and selectivity for quantifying URI level is extremely desirable.

In this paper, we presented the electropolymerization of Blue HEGN dye (Scheme 1) on the surface of GCE (Po- BHEGN/GCE) using CV techniques. There were no published reports on Blue HEGN's modification on GCE for the detection of URI. As a result, in this paper, we constructed simple and less-cost Po-BHEGN/GCE and characterized its electrochemical properties. At pH 7.4, Po-BHEGN/GCE exhibited an adequate response in the interference-free detection of URI in the existence of DA by DPV methods. The findings of this work have substantial implications for electroanalytical chemistry and sensors.

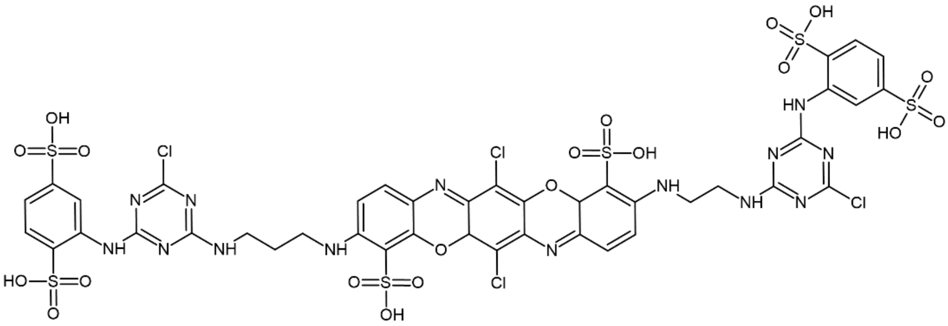

Scheme 1. Structure of Blue HEGN

2. EXPERIMENTAL PART

2.1. Apparatus, chemicals, and reagents

The voltammetric measurements were taken with a model CHI-660C (CH instrument -660 electrochemical workstation). The three-electrode cell configuration, features a glassy carbon working electrode, a saturated calomel reference electrode, and a Pt counter electrode. Nice chemicals supplied URI, DA, Na_2HPO_4, NaH_2PO_4, and NaOH. Astik Dyestuffs Pvt. Ltd, Gujarath provided Blue HEGN dye. All of the chemicals used in the experiment were utilized unprocessed. All of the solutions are made with Double distilled water. 0.2M PBS was made by mixing a sufficient quantity of Na_2HPO_4 and NaH_2PO_4.

2.2. Setup of GCE and Po-BHEGN/GCE

The GCE, which was used as a working electrode through all experiments was manually polished with alumina (0.05 µm) powder.

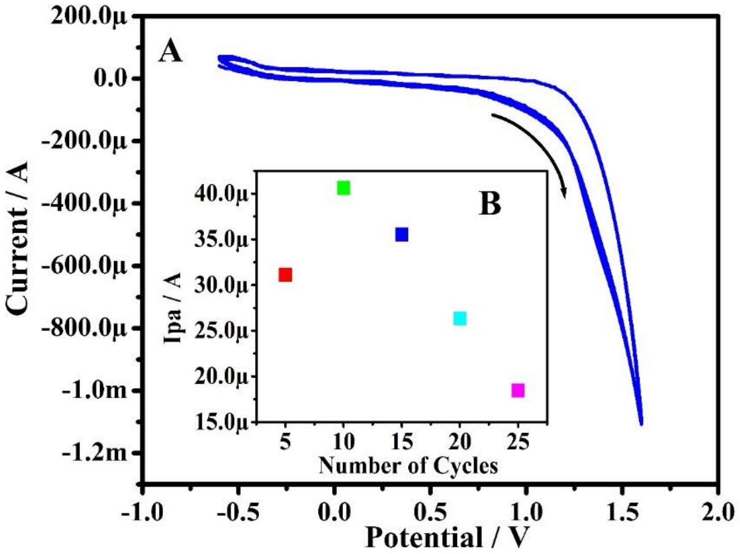

Figure 1 a) CVs of construction of Po-BHEGN/GCE in 0.1 M NaOH at 10 sweep rates; b) Graph of I_{pa} *vs.* number of cycles

Eventually rinsed with de-ionized water after polishing. The Po-BHEGN/GCE was fabricated by electropolymerization of 0.1 mM Blue HEGN dye in 0.1 M NaOH as a supporting electrolyte on the GCE surface using CV techniques. According to Figure 1A, a potential zone of -0.6 to +1.7 V was used for the electropolymerization with a sweep rate (SR) of 100 mV/s at 10 cycles.

3. RESULTS AND DISCUSSION

3.1. Characterization and electroactive surface area of Po-BHEGN/GCE

The thickness of the polymer layer has a considerable impact on the electrocatalytic properties of Po-BHEGN/GCE. The Po-BHEGN/GCED layer thickness can be strongly suppressed by altering the number of sweep segments from 5 to 25. From Figure 1B, we found an elevated oxidation peak current of URI from 5-10 segments; however, from 10-25 segments, the URI oxidation peak current steadily declined, which is most likely owing to adequate coverage of Po-BHEGN layer on the available GCE surface area. Ten sweep segments give appropriate coverage on the Po-BHEGN/GCE. As a consequence, 10 sweep segments were recognized as the best for this experiment.

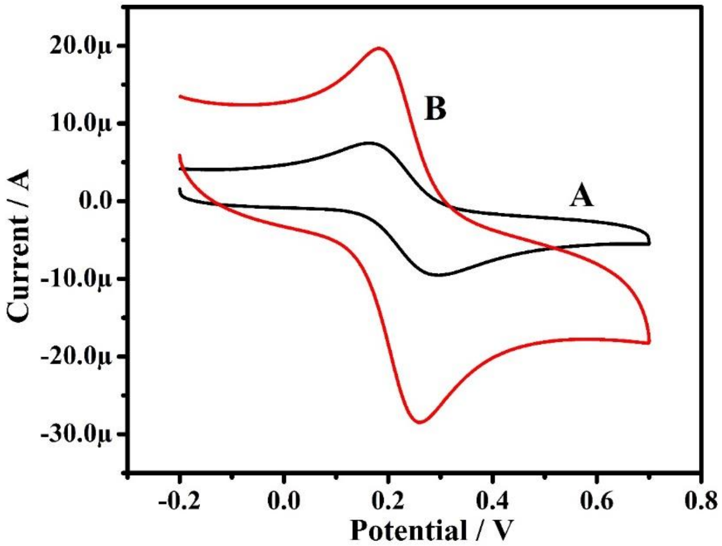

Figure 2. CVs of 1 mM of $K_4[Fe(CN)_6]$ in KCl (1.0 M) at GCE (curve A) and Po-BHEGN/GCE (curve B) at a sweep rate of 100 mV/s

CV was used to investigate the electrolytic interaction between Po-BHEGN/GCE and URI, with $K_4[Fe(CN)_6]$ (1.0 mM) as a redox system containing supporting electrolyte KCl (1.0 M) at SR of 100 mV/s. The CV of Figure 2 reveals that Po-BHEGN/GCE (curve B) has a much-amplified I_{pa} (28.76 µA) in contrast to GCE (curve A), which has a lower I_{pa} value (9.50 µA). This rise in I_{pa} of Po-BHEGN/GCE is attributed to the fact that there are more electroactive sites as a result of the growth of the thin layer of Blue HEGN on the electrode's exterior and hence facilitates speed up of electron transfer. The electroactive surface area of GCE and Po-BHEGN/GCE is calculated using the Randels-Sevick equation [30–32]:

$$I_{pa} = (2.69\times10^{-5})\, n^{3/2}\, C_0\, A\, D^{1/2}\, \upsilon^{1/2} \qquad (1)$$

where n is the number of electrons involved, Ipa is the peak current, A is surface area, and υ is the sweep rate. C_0 and D are the electroactive species concentration and diffusion coefficient respectively. The electroactive surface area of Po-BHEGN/GCE (0. 0412 cm^2) is nearly twice that of GCE (0.0248 cm^2), indicating that it is solid evidence for the productive and constructive modification of GCE by a polymer layer of Blue HEGN.

3.2. Voltammetric response of URI at Po-BHEGN/GCE

The cyclic voltammograms for 0.1 mM URI in 0.2 M PBS (7.4 pH) at SR of 100 mV/s are illustrated in Figure 3. The CV for GCE (dashed curve A) has quite a low oxidation peak current response and is noticed at 0.28 V with a broad voltammogram. The CV produced for Po-BHEGN/GCE (solid curve B) displays a high oxidation peak current with a keen voltammogram at 0.25 V. Therefore, the Po-BHEGN/GCE is more vulnerable to URI oxidation than CGE.

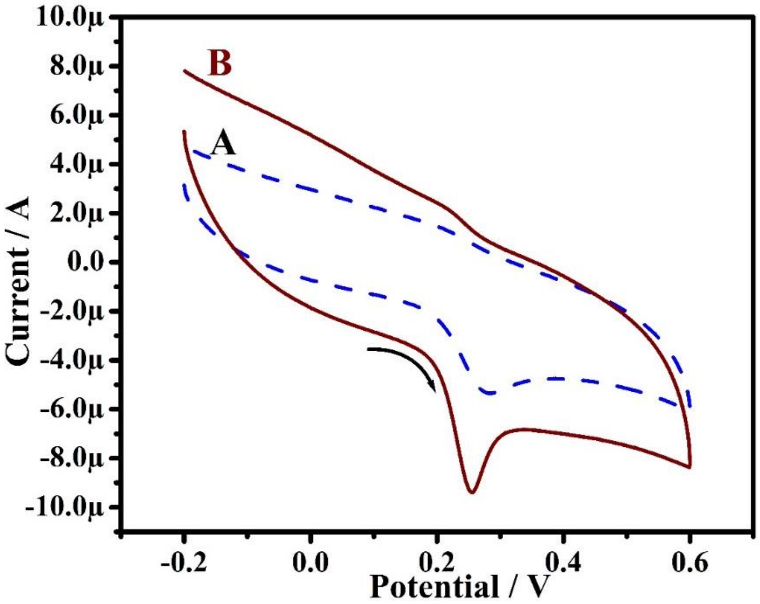

Figure 3. CVs of 0.1 mM URI in 0.2 M PBS (7.4 pH) at GCE (dashed curve A) and Po-BHEGN/GCE (solid curve B) at sweep rate 100 mV/s

3.3. Effect of sweep rate

The analysis of CVs of URI at various sweep rates revealed information on the influence of peak current on sweep rate and even the type of electrode process occurring at the electrode surface. The CVS (Figure 4A) produced for the analysis of 0.1mM URI in 0.2M PBS (7.4 pH) on Po-BHEGN/GCE indicate that the I_{pa} is proportional to sweep rate, demonstrating electron transport between the Po-BHEGN/GCE and URI. The I_{pa} is seen to move to the positive side as the sweep rate grows from 50-500 mV/s. The graphs of I_{pa} VS υ (Figure 4B) and I_{pa} *vs.* $\upsilon^{1/2}$ (Figure 4C) suggested that the process is diffusion controlled [33]. Since they are linear with correlation coefficients 0.994 and 0.998 respectively, and linear regression expressions I_{pa} (µA) = 0.16 υ (m V/s) + 27.02 and I_{pa} (µA) = 4.97 $\upsilon^{1/2}$ (mV/s) – 6.93, respectively.

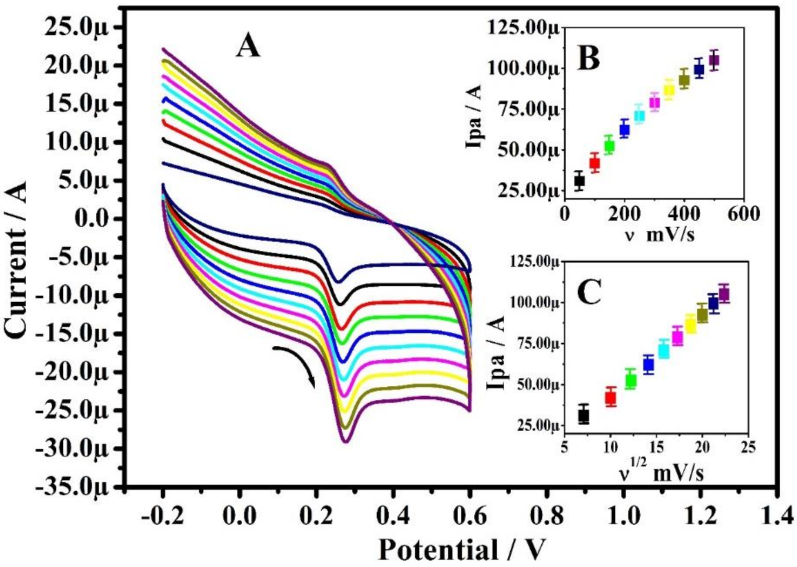

Figure 4. a) CVs of 0.1 mM URI at Po-BHEGN/GCE at sweep rate from 50-500 mV/s; b) Graph of I_{pa} *vs.* υ mV/s; c) Graph of I_{pa} *vs.* $\upsilon^{1/2}$ mV/s

3.4. pH study

The buffer's pH plays an essential role in modulating the mechanism of electrochemical performance of URI at Po-BHEGN/GCE. The CVs produced on 0.1 mM UAC by elevating the pH from 6.2 to 7.8 appears in Figure 5A, and it clears that when pH rises, the peak potential switches to the negative potential. The linearity between E_{pa} and pH in Figure 5B is given by the linear regression expression E_{pa} (mV/s) = -0.06 pH + 0.75 (R^2= 0.999), which describes the same number of electrons and protons engaged in the oxidation process (Scheme 2) [34].

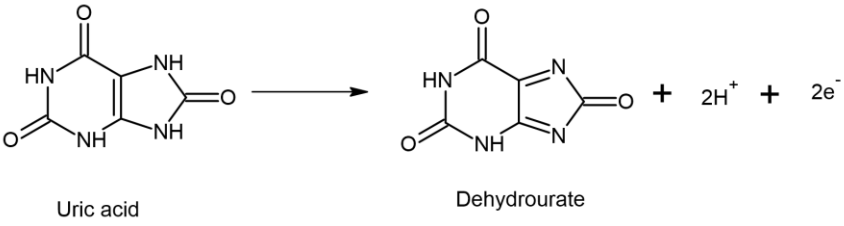

Scheme 2. Electrochemical oxidation of URI

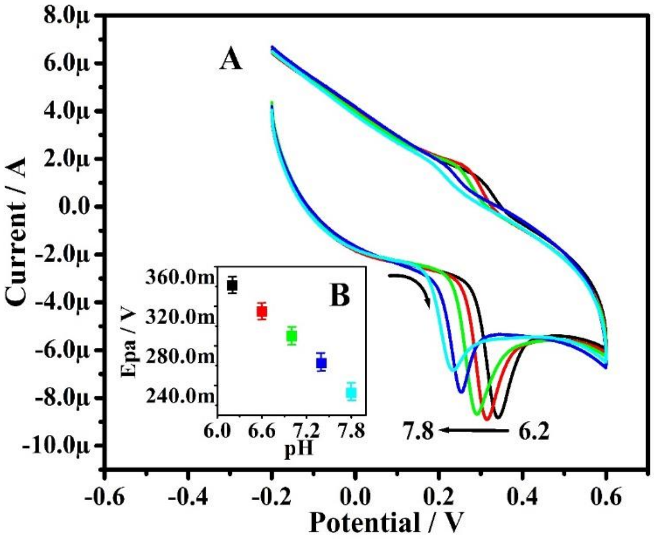

Figure 5. a) CVs obtained for varied pH at Po-BHEGN/GCE; b) Graph of E_{pa} *vs.* pH

3.5. Detection limit and quantification studies of URI at Po-BHEGN/GCE

Figure 6A presents CVs of URI at Po-BHEGN/GCE in the concentration range of 10µM - 70µM. Where the peak current grows as the URI concentration grows. Linearity is evident in the graph of I_{pa} VS URI concentrations (I_{pa} (µA) = 0.49 [URI] (µM) + 3.35 (R^2=0.999)) (Figure 6B). LOD and LOQ (LOD = 3S/M, LOQ = 10S/M, where S and M stands for standard deviation and slope of the graph) were determined from the collected data to be 0.94 and 3.15 µM, respectively. Table 1 compares the LOD of URI at Po-BHEGN/GCE to other works published in the literature.

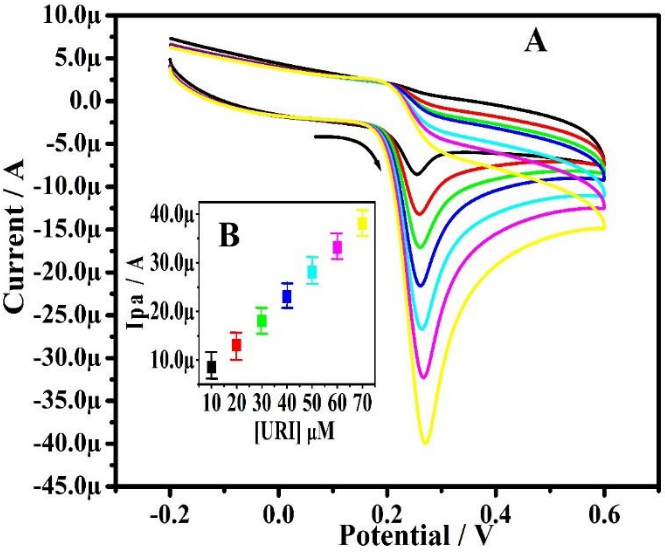

Figure 6. a) CVs of increased URI concentrations (10-70 µM) at Po-BHEGN/GCE; b) Graph of I_{pa} *vs.* URI concentration

Table 1. Comparison of LOD of URI at Po-BHEGN/GCE with previously reported sensors

Sl. No	Electrode	LOD of URI (µM)	Method	References
1	Poly (*o*-aminophenol)-MCPE	3.0	CV	[11]
2	Pd/RGO/GCE	1.6	DPV	[35]
3	Glu/GCE	1.1	DPV	[36]
4	Au-Cu_2O/rGo/GCE	6.5	DPV	[37]
5	Pdop@GR/MWCNTs	15.0	DPV	[38]
6	PG/GCE	4.82	CV	[39]
7	PPS/SAOS/MCPE	4.18	CV	[40]
8	Po-BHEGN/GCE	0.94	CV	Present work

3.6. Simultaneous analysis of URI and DA

The CV techniques were adopted to explore 0.1 µM URI and DA mixture in 0.2 M PBS (7.4, pH) on the Po-BHEGN/GCE surface (curve B) and GCE (curve A) (Figure 7). Curve B depicts well-defined electrooxidation peaks caused by URI and DA with an increase in I_{pa} at peak potentials of 0.271 and 0.126 V, correspondingly in the exclusion of baseline current. Furthermore, for GCE, the unique peak split up for URI and DA is not certain. As a result, Po-BHEGN/GCE is a sensitive sensor for novel and selective evaluation of URI in occurrence with DA.

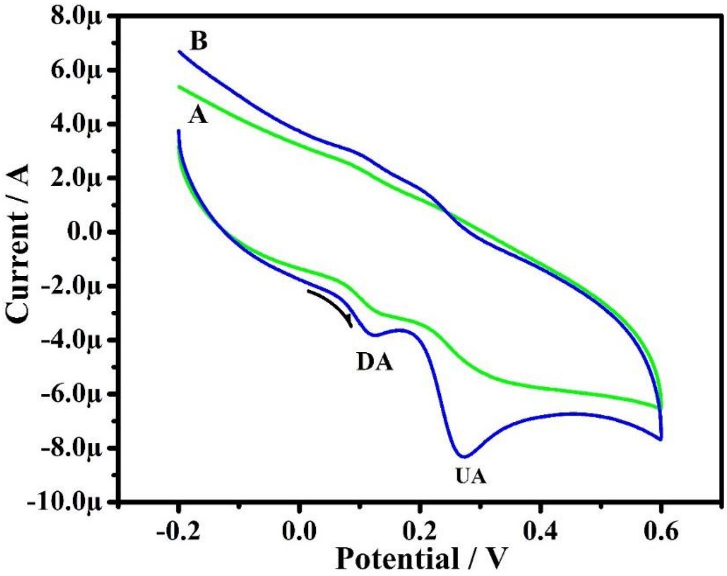

Figure 7. CVs of simultaneous studies of URI and DA at GCE (curve A) and Po-BHEGN/GCE (curve B) at a sweep rate of 100 mV/s

3.7. Interference studies

Interference studies were performed by combining URI and DA in 0.2 M PBS (7.4 pH) at Po-BHEGN/GCE using DPV techniques. Since URI and DA have unique actions in living beings, the action of URI and DA in the composite form was investigated to determine whether the electrocatalytic potential of the proposed Po-BHEGN/GCE towards URI is comparable. The levels of one specimen are altered while the levels of another specimen are kept static and vise-versa. Figure 8 demonstrates that only the DA peak current was enhanced by raising the DA levels from 10-70 µM while preserving the URI level constant. Figure 9 shows that only the URI peak current was raised by varying the URI levels from 10-60 µM while maintaining the DA levels constant. These results imply that the interference of DA did not affect the electrochemical behaviors of URI. In conclusion, the suggested model and Po-BHEGN/GCE are virtually free of interference.

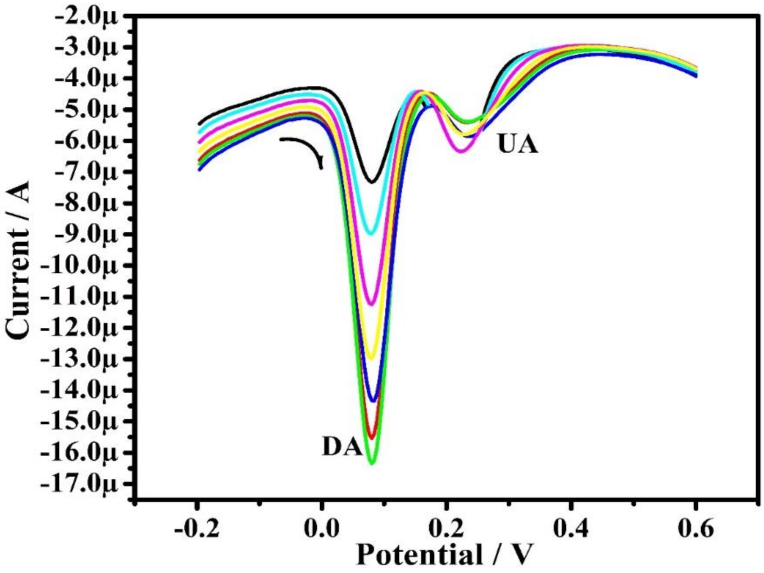

Figure 8. DPVs of varied concentrations of DA (10-70 µM) at a static concentration of URI

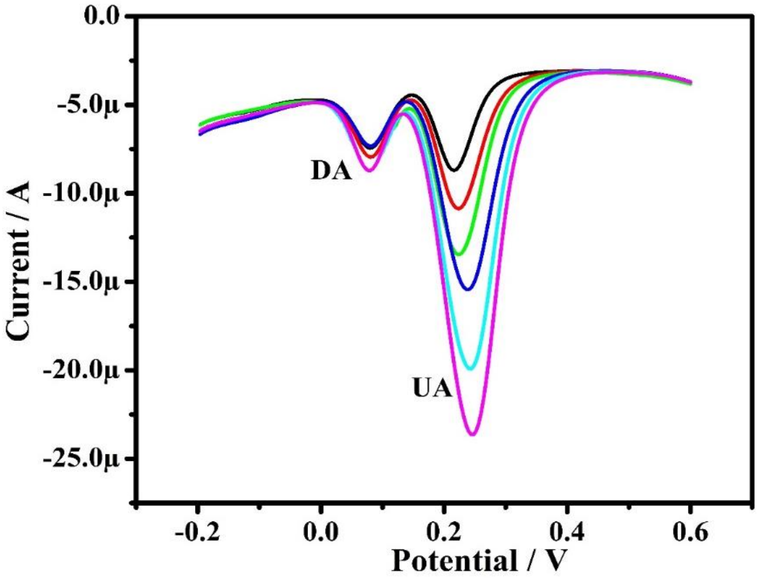

Figure 9. DPVs of varied concentrations of URI (10-60 µM) at a static concentration of DA

3.8. Reproducibility, repeatability, and stability

When the reproducibility of the Po-BHEGN/GCE was verified after 6 days, it was discovered that the peak current signal recovered 97.4% of the initial start-up current response and had no effect on the peak potential. The repeatability of the Po-BHEGN/GCE was checked by performing four consecutive CV cycles, and the results show excellent repeatability with an RSD value of 3.96. Sweeping 20 consecutive cycles to test the stability of the Po-BHEGN/GCE revealed that 96.4% of the initial current is preserved even after 20 cycles.

3.9. Analysis of URI in Urine sample

The Po-BHEGN/GCE was used to measure URI in a urine sample in 0.2M PBS 97.4 pH). When a known amount of URI (10µM) was injected into real samples, the standard addition approaches provided quantitative recovery ranging from 97.7 to 99.1% (Table 2). These appealing characteristics of the Po-BHEGN/GCE point to a possible application for assaying URI in physiological situations.

Table 2. Detection of URI in a urine sample

Sample	Added URI (µM)	Estimated URI (µM)	% Recovery
Urine	10	9.7	97.7± 2
	20	19.6	96.4± 3
	30	29.5	99.1± 2

4. CONCLUSION

In this work, Po-BHEGN/GCE an effective electroanalytical tool was fabricated by simply modifying a GCE with Blue HEGN dye by electropolymerization method via CV techniques. The major purpose of this study was to determine whether a Po-BHEGN/GCE could be used to quickly screen URI. A linear response between 10-70 µM for URI with a detection limit of 0.94 µM was obtained. In simultaneous studies, the Po-BHEGN/GCE demonstrated excellent performance in the assay of URI in occurrence with DA. The interference study suggested that Po-BHEGN/GCE is free of any interferences. The developed Po-BHEGN/GCE fared better recovery in the urine sample. These attractive features concluded that the Po-BHEGN/GCE is the more promising and potent sensor in the study of other biologically active molecules and pharmaceutical samples.

Conflict of Interest

The authors declare that they have no conflicts of interest.

REFERENCES

[1] H. Yao, Y. Sun, X. Lin, Y. Tang, A. Liu, G. Li, W. Li, and S. Zhang, Anal. Sci. 23 (2007) 677.

[2] M. Shabani-Nooshabadi, and M. Roostaee, J. Mol. Liq. 220 (2016) 329.

[3] P. S. Ganesh, G. Shimoga, S. H. Lee, S. Y. Kim, and E. E. Ebenso, ChemistrySelect 6 (2021) 2379.

[4] M. Ławrywianiec, J. Smajdor, B. Paczosa-Bator, and R. Piech, Anal. Methods 9 (2017) 6662.

[5] T. Kokab, A. Shah, J. Nisar, A. M. Khan, S. B. Khan, and A. H. Shah, ACS Omega 5 (2020) 10123.

[6] A. M. Abdel-Aziz, H. H. Hassan, and I. H. A. Badr, Anal. Chem. 92 (2020) 7947.

[7] R. Jerome, and A. K. Sundramoorthy, J. Electrochem. Soc. 166 (2019) 3017.

[8] S. A. Kumar, C. F. Tang, and S. M. Chen, Talanta, 76 (2008) 997.

[9] V. Mani, M. Govindasamy, S. M. Chen, R. Karthik, and S. T. Huang, Microchim. Acta 183 (2016) 2267.

[10] S. B. Khoo, and F. Chen, Anal. Chem. 74 (2002) 5734.

[11] E. Miland, A. Mirandaordieres, P. Tunonblanco, M. Smyth, and C. Fagain, Talanta 43 (1996) 785.

[12] D. G. Dilgin, D. Gligor, H. I. Gökçel, Z. Dursun, and Y. Dilgin, Microchim. Acta 173 (2011) 469.

[13] P. S. Ganesh, G. Shimoga, S. H. Lee, S. Y. Kim, and E. E. Ebenso, J. Anal. Sci. Technol. 12 (2021) 20.

[14] A. A. Kumar, T. S. Rani, P. S. Ganesh, and B. E. K. Swamy, Anal. Bioanal. Electrochem. 9 (2017) 328.

[15] A. Hammoud, D. Chhin, D. K. Nguyen, and M. Sawan, Biosens. Bioelectron., 180 (2021) 113089.

[16] O. E. Fayemi, A. S. Adekunle, B. E. K. Swamy, and E. E. Ebenso, J. Electroanal. Chem. 818 (2018) 236.

[17] T. S. Thanh, P. T. Qui, N. T. T. Tu, T. T. T. Toan, T. T. B. Hoa, L. V. T. Son, D. M. Nguyen, T. N. Tugen, and D. Q. Khieu., J. Nanomater. 2021 (2021) 9914062.

[18] H. Kaur, and B. Halliwell, Chem. Biol. Interact. 73 (1990) 235.

[19] N. T. V. Hoan, N. N. Minch, N. T. H. Trang, L. T. T. Thung, C. V. Hoang, T. X. Mau, H. X. A. Vu, P. T. K. Thu, N. H. Phong, and D. Q. Khieu, J. Nanomater. 2020 (2020) 9797509.

[20] Y. J. Chang, M. C. Lee, and Y. C. Chien, SLAS Technol. 27(2022)54.

[21] D. Plausinaitis, L. Sinkevicius, U. Samukaite-Bubniene, V. Ratautaite, and A. Ramanavicius, Talanta 220 (2020) 121414.

[22] I. Grabowska, M. Chudy, A. Dybko, and Z. Brzozka, Sens. Actuators B 130 (2008) 508.

[23] M. Pucetaite, M. Velicka, J. Pilipavicius, A. Beganskiene, J. Ceponkus, and V. Sablinskas, J. Raman Spec. 47 (2016) 681.

[24] B. Demirkan, S. Bozkurt, K. Cellat, K. Arikan, M. Yilmaz, A. Sark, M. H. Calimli, M. S. Nas, M. N. Atalar, and M.H. Alma, Sci. Rep. 10 (2020) 2946.

[25] D. Ortiz-Aguayo, M. Bonet-San-Emeterio, and M. del Valle, Sensors 19 (2019) 3286.

[26] C. R. Raj, F. Kitamura, and T. Ohsaka, Analyst 127 (2002) 1155.

[27] B. Han, M. Pan, X. Liu, J. Liu, T. Cui, and Q. Chen, Materials 12 (2019) 214.

[28] Y. Yang, M. Li, and Z. Zhu, Talanta 201 (2019) 295.

[29] S. B. Tanuja, B. E. K. Swamy, and P. K, Vasanthkumar, J. Anal. Bioanal. Tech. 7 (2016) 1000297.

[30] T. Dhanasekaran, R. Manigandan, A. Padmanaban, R. Suresh, K. Giribabu, and V. Narayanan, Sci. Rep. 9 (2019) 13250.

[31] B. Mekassa, M. Tessema, B. S. Chandravanshi, P. G. L. Baker, and F. N. Muya, J. Electroanal. Chem. 807 (2017) 145.

[32] S. Deepa, B. E. K. Swamy, K. V. Pai, and K. R. Mahanthesha, Anal. Bioanal. Electrochem. 11 (2019) 1240.

[33] D. Majer, and M. Finšgar, Biosensors 11 (2021) 285.

[34] R. Sainz, M. del Pozo, M. Vilas-Varela, J. Castro-Esteban, M. P. Corral, L. Vázquez, E. Blanco, D. Peña, J. A. Martín-Gago, G. J. Ellis, M. D. Petit-Domínguez, C. Quintana, and E. Casero, Sci. Rep. 10 (2020) 14614.

[35] J. Wang, B. Yang, J. Zhong, B. Yan, K. Zhang, C. Zhai, Y. Shiraishi, Y. Du, and P. Yang, J. Colloid Interface Sci. 497 (2017) 172.

[36] L. Zhang, and X. Lin, Analyst 126 (2001) 367.

[37] T. K. Aparna, R. Sivasubramanian, and M. A. Dar, J. Alloys Compd. 741 (2018)1130.

[38] C. Wang, J. Li, K. Shi, Q. Wang, X. Zhao, Z. Xiong, X. Zou, and Y. Wang, J. Electroanal. Chem. 770 (2016) 56.

[39] S. Qi, B. Zhao, H. Tang, and X. Jiang, Electrochim. Acta 161 (2015) 395.

[40] T. S. N. S. K. Naik, and B. E. K. Swamy, Anal. Bioanal. Electrochem. 9 (2017) 424.